DALTON
FULL PAPER

Structure of lithium–*p*-semiquinonates in non-aqueous solution*

Martyn A. Brown, Bruce R. McGarvey and Dennis G. Tuck

Department of Chemistry and Biochemistry, University of Windsor, Windsor, Ontario, N9B 3P4, Canada

The reaction of phenyllithium with *p*-quinones (1,4-benzoquinone, 2,6-di-*tert*-butyl-1,4-benzoquinone, 1,4-naphthoquinone) in tetrahydrofuran gave the phenyl radical, which goes to biphenyl, and the corresponding lithium semiquinonate. The latter can also be obtained by direct reaction between lithium and the *p*-quinone. Electron spin resonance spectroscopy showed that a solution of the lithium derivative contains both monomeric and dimeric species. Adducts with 4-methylpyridine have also been prepared. Quantum-mechanical calculations were consistent with the ESR results. Related experiments with potassium derivatives were also performed.

We recently showed that phenyllithium can be oxidised in non-aqueous media by various substituted orthoquinones to give the corresponding lithium *o*-semiquinonates.[1] This one of the simplest reactions in which an *o*-quinone oxidises an organic moiety, and has important consequences in the redox chemistry of organometallic compounds.[2] The same paper also showed that the resultant $Li^+(sq^{\bullet -})$ species (sq = semiquinone) are associated in solution, and the identification of trimeric entities by electron spin resonance (ESR) spectroscopy was supported by molecular orbital modelling results.

In the light of these results, and of continuing studies in this laboratory on the interactions of *o*- and *p*-quinones with complexes of Main Group elements, we have now investigated the reaction of phenyllithium with *p*-quinones. The products are again $Li^+(sq^{\bullet -})$ species, but ESR spectroscopy demonstrates the presence of dimers in non-aqueous solution. Calculations give structural and thermodynamic results which are consistent with the ESR spectra.

Experimental

Metals (Li, K) were cut into suitable sizes from the commercially available material (Aldrich). Phenyllithium, *p*-quinones, 4-methylpyridine (picoline, pic) and pyridine were used as supplied (Aldrich). Solvents were dried, redistilled and degassed before use. Microanalysis was by Canadian Microanalytical Services. Mass spectra were recorded on a Shimadzu 14-B instrument operating in the EI mode, with Sun Sparc software, and infrared spectra for KBr discs in a Nicolet 5DX instrument. All experiments were carried out in an atmosphere of dry nitrogen, using conventional vacuum-line techniques.

Electron spin resonance spectroscopy

Spectra were recorded in the X-band region on a Bruker ESP-300E instrument, calibrated against a Bruker nuclear magnetometer and a Hewlett-Packard microwave frequency counter. A liquid-nitrogen-cooled cavity insert allowed spectra to be measured to 77 K. The operating frequencies were *ca.* 9.77 GHz at room temperature and 9.44 GHz at 77 K. Simulation of experimental spectra was by the Symphonia program (Bruker).

Preparation of Li^+ $(sq^{\bullet -})$ compounds

(i) In a typical experiment, a stirred solution of the *p*-quinone (0.01 mol) in tetrahydrofuran (20 cm^3) was treated with an equimolar quantity of PhLi in diethyl ether–cyclohexane (70:30) at room temperature. An immediate colour change indicated a rapid reaction. Solid products were obtained by removing *ca.* 50% of the solvents *in vacuo*, followed by cooling to 0 °C. Analytical results for these, and other materials, are given in Table 1. In two cases the addition of an excess of 4-methylpyridine to a portion of the reaction mixture led to the formation of adducts of the type $Li(sq)(pic)_2$; in neither case were we able to obtain crystals of sufficient quality for X-ray analysis.

(ii) The semiquinonate derivatives of lithium, and in two cases potassium, could also be readily obtained by refluxing the metal and *p*-quinone together in toluene. The lithium compounds were analytically and spectroscopically identical with those obtained by starting with PhLi.

Modelling procedures

Since the ESR results indicated the existence of dimeric species in solution we attempted to model the structures of Li^+-$(p\text{-}C_6H_4O_2^{\bullet -})$ and its dimer. Quantum-mechanical calculations were performed using a modification of the AM1 molecular modelling program of Dewar *et al.*,[3] running on a personal computer. This program has been shown to reproduce satisfactorily experimental values of bond distances and angles, and enthalpies of formation, of small molecules. Charge distributions can also be calculated. Bond distances are quoted to 0.001 Å, angles to 1°, and electronic charges to 0.001; these limits probably overstate the absolute accuracy of the calculations, but the main thrust of the argument is in terms of comparisons between related species, and such comparisons are more meaningful than the individual values.

Results and Discussion

Preparative

The reaction between alkali metals and quinones has long been known to yield the semiquinonate compounds, and we have now shown that the redox process (2) occurs for both *o*-[1] and *p*-quinones. As in the earlier work, the formation of $Ph^\bullet$ radicals was confirmed by identifying biphenyl in the reaction solution by mass spectrometry.

$$M + q \longrightarrow M^+(sq^{\bullet -}) \qquad (1)$$

$$PhLi + q \longrightarrow Li^+(sq^{\bullet -}) + Ph^\bullet \qquad (2)$$

Electron spin resonance spectroscopy

The ESR spectrum of a concentrated solution of $Li^+(p\text{-}C_6H_4O_2^{\bullet -})$ in toluene at room temperature, and of the other

---

* *Non-SI unit employed*: G = 10^{-4} T.

Table 1 Analytical results, with calculated values in parentheses, for lithium–*p*-quinone derivatives

Reaction	Product	Colour	Analysis (%)	
			C	H
Li + p-C$_6$H$_4$O$_2$	Li(p-C$_6$H$_4$O$_2$)	Blue	62.9 (62.6)	3.60 (3.50)
K + p-C$_6$H$_4$O$_2$	K(p-C$_6$H$_4$O$_2$)	Green	49.2 (49.0)	2.35 (2.70)
Li + *p*-dtbq[a]	Li(p-C$_6$H$_4$O$_2$)	Brown	74.9 (74.0)	8.10 (8.80)
PhLi + *p*-dtbq	Li(*p*-dtbsq)	Brown	74.6 (74.0)	8.65 (8.80)
Li + *p*-dtbq + pic	Li(*p*-dtbsq)-(pic)$_2$	Brown	74.9 (75.5)	7.95 (8.25)
Li + *p*-nq[b]	Li(*p*-nsq)	Black	72.0 (72.7)	3.75 (3.65)
PhLi + *p*-nq	Li(*p*-nsq)	Black	72.6 (72.7)	3.60 (3.65)
PhLi + *p*-nq + pic	Li(*p*-nsq)-(pic)$_2$	Black	76.4 (75.2)	6.25 (5.70)

[a] *p*-dtbq = 2,6-Di-*tert*-butyl-1,4-benzoquinone. [b] *p*-nq = 1,4-Naphthoquinone.

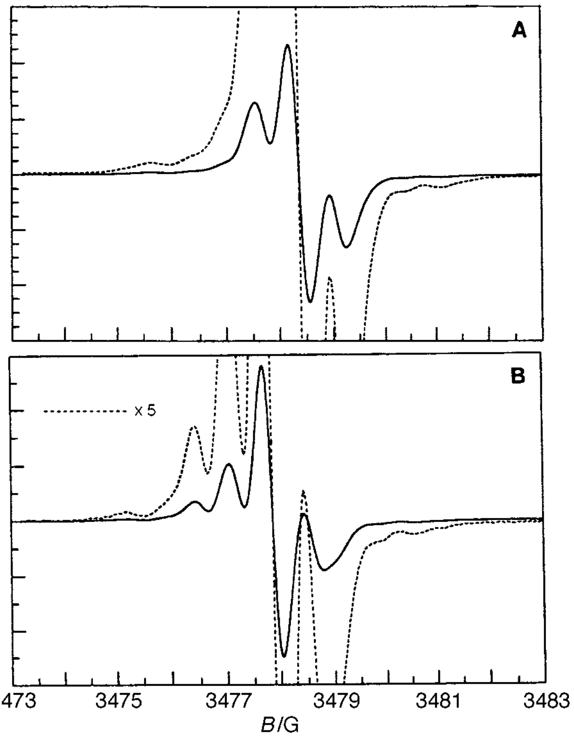

Fig. 1 The ESR spectra of a dilute solution of $\mathrm{Li^+}(p\text{-}\mathrm{C_6H_4O_2}^{\cdot-})$ at room temperature (A) and of the same solution containing picoline (B)

lithium *p*-semiquinonates studied, is a broad featureless singlet. On dilution these solutions give various multiline patterns, some of which are anisotropic in shape. Fig. 1A shows the spectrum of $\mathrm{Li^+}(p\text{-}\mathrm{C_6H_4O_2}^{\cdot-})$, and Fig. 1B that of the same solution following the addition of picoline. Weaker additional lines are seen in the baseline when the gain is increased. The hyperfine spacings are approximately 0.6 G in both cases. Similar three- and five-line spectra are seen when potassium is substituted for lithium, although the spectra are more symmetrical and the hyperfine spacing is now about 1.5 G. In fact the spectrum for the sample containing picoline can be satisfactorily simulated on the basis of four equivalent protons, similar to that of the free semiquinone radical,[4] except that the hyperfine splitting is 60% of that found for the free semiquinone. Well resolved spectra could not be obtained for dilute solutions of $\mathrm{Li^+}(p\text{-dtbsq}^{\cdot-})$, with or without addition of pyridine. In the case of $\mathrm{Li^+}(p\text{-nsq}^{\cdot-})$ a complex pattern of hyperfine lines was observed, and on the addition of picoline the spectrum became anisotropic, with additional lines. With the exception of $\mathrm{K^+}(p\text{-}\mathrm{C_6H_4O_2}^{\cdot-})$ plus picoline, no acceptable simulation

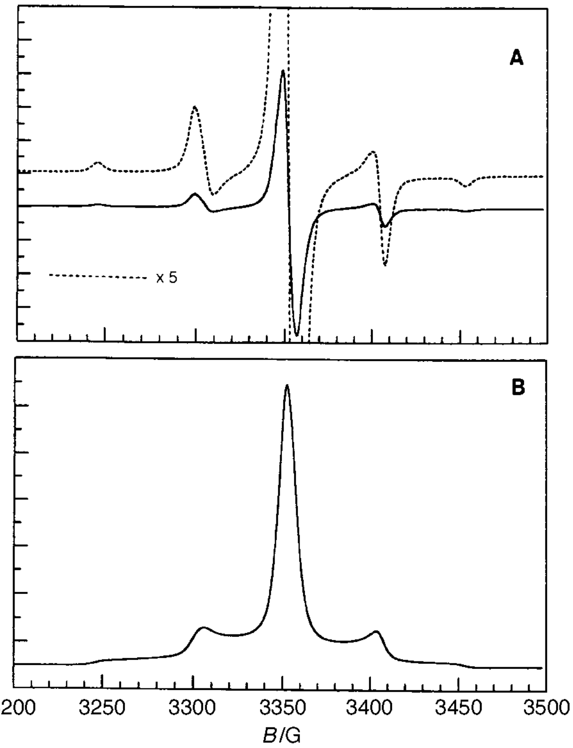

Fig. 2 (A) The ESR spectrum of a frozen solution of $\mathrm{Li^+}(p\text{-}\mathrm{C_6H_4O_2}^{\cdot-})$ at 77 K, (B) the absorption ESR spectrum obtained by integrating (A)

was found for the room-temperature spectra of these dilute solutions.

The inability to simulate most of the room-temperature spectra of dilute solutions is due to the presence of more than one species, plus the incomplete averaging of the *g* and hyperfine matrices which produces the asymmetrical spectra observed. Our experience with other complexes of Main Group metal ions with semiquinones has shown that the addition of a ligand which binds strongly at vacant co-ordination sites, such as picoline, produces a simpler spectrum and this is the case here, where the expected five-line pattern is dominant. The splitting observed in each spectrum must be due to the hyperfine interaction with the ring proton in the benzosemiquinone. Methyl and chloro substitution in the ring of the benzosemiquinone anion has been shown[4] to give values of the hyperfine constant ranging from 1.7 to 2.5 G. These measurements were made in alkaline solutions with polar solvents and a decrease in the pH produces[5] more complex spectra as the anion is converted into the weak acid. Our solvent is non-polar and we expect to find not the free anion, but rather an ion pair. The very small hyperfine constant, 0.6 G, observed for $\mathrm{Li^+}(p\text{-}\mathrm{C_6H_4O_2}^{\cdot-})$ and the somewhat small constant, 1.5 G, for $\mathrm{K^-}(p\text{-}\mathrm{C_6H_4O_2}^{\cdot-})$ indicate that the cation is bound to one of the oxygen atoms, and this draws the unpaired electron onto the oxygen atom, reducing the spin density on the carbon atoms bonded to the hydrogen atoms. This is consistent with the results of modelling calculations (see below) which imply that the Li–*p*-sq interaction involves a Li–O bond similar to that in many other stable lithium complexes, and that there is substantial polarity in the >C–O–Li part of the molecule.

The ESR spectrum of a frozen (77 K) concentrated solution of $\mathrm{Li^+}(p\text{-}\mathrm{C_6H_4O_2}^{\cdot-})$ shown in Fig. 2A, along with the integrated spectrum in Fig. 2B, is typical of an $S = 1$ plus an $S = \frac{1}{2}$ mixture. A strong resonance was also detected at half-field, confirming the presence of the $S = 1$ system. This indicates the presence of dimeric as well as monomeric species in the concentrated solution. Such oligomerisation is similar to that observed for lithium–*o*-quinone systems, with the important quantitative difference that in the present work no weakly coupled trimers

Table 2 ESR Parameters of $S = 1$ species in frozen solutions of metal–*p*-quinones

Solution	g_x	g_y	g_z	D/G	E/G	$I_{\text{dimer}}/I_{\text{monomer}}$
$Li^+(p\text{-}C_6H_4O_2{}^{\bullet -})$	2.006	2.007	2.0095	104	2	1
$Li^+(p\text{-}C_6H_4O_2{}^{\bullet -})$ + pic	2.006	2.007	2.0095	108	1	1.06
$Li^+(p\text{-dtbsq}^{\bullet -})$ + pic	2.004	2.004	2.0065	108	1	1.40
$K^+(p\text{-}C_6H_4O_2{}^{\bullet -})$	2.007	2.007	2.007	89, 82, 73, 65	—	1

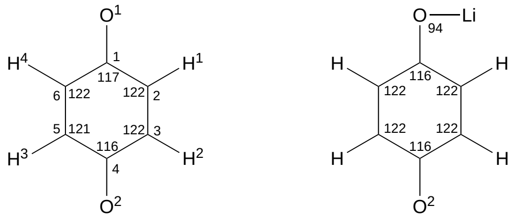

Scheme 1

were detected. Similar spectra were observed when an excess of picoline was present. For frozen solutions of $Li^+(p\text{-dtbsq}^{\bullet -})$ a much broader $S = 1$ species was observed, but the addition of an excess of picoline produced a sharper spectrum, similar to that shown in Fig. 2. In the case of $K^+(p\text{-dtbsq}^{\bullet -})$ at least four distinct $S = 1$ spectra could be identified in the frozen-solution spectrum, but the addition of picoline gave a broad spectrum in the $S = 1$ region, and a weak half-field resonance was detected. For frozen solutions of $Li^+(p\text{-nsq}^{\bullet -})$ a weak half-field resonance indicated the presence of $S = 1$ species, but no corresponding resonance from this species could be detected in the $g = 2$ region.

The $S = 1$ spectra were simulated using the spin Hamiltonian (3) and the results are in Table 2. In those cases where a good

$$H = \beta(g_xB_xS_x + g_yB_yS_y + g_zB_zS_z) + D[S_z{}^2 - \tfrac{1}{3}S(S + 1)] + E(S_x{}^2 - S_y{}^2) \quad (3)$$

integration of the derivative spectrum could be made, we estimated the ratio of the intensity of the dimer to that of the monomer, and this is also given. Any interpretation of this ratio must be done with care, since $\Delta M_s = \pm 1$ transitions in $S = 1$ systems are fundamentally twice as intense as those for $S = \frac{1}{2}$ systems and the $S = 1$ system exists in both the triplet state, which was detected, and the singlet state, which we did not detect. If we assume that the exchange energy which separates the singlet and triplet states is small compared to the thermal energy kT, such that $\frac{3}{4}$ of the dimer is in the triplet state and $\frac{1}{4}$ in the singlet state, it can be shown that the ratio of dimers to monomers in the mixture is given by equation (4). We consider

$$\frac{N_{\text{dimer}}}{N_{\text{monomer}}} = \frac{I_{\text{dimer}}}{2I_{\text{monomer}}} \quad (4)$$

this ratio to be essentially that of the room-temperature solution, since the solutions were frozen rapidly by direct immersion in liquid nitrogen. In most solutions we estimate that about 50 mol% of the metal *p*-semiquinones were present as the dimer.

Table 3 Calculated bond distances (Å), charge distributions, and enthalpies of formation (kJ mol^{-1}) for $p\text{-}C_6H_4O_2$ and $Li^+(p\text{-}C_6H_4O_2{}^{\bullet -})$; numbering system and bond angles (°) in Scheme 1

	$p\text{-}C_6H_4O_2$	$Li^+(p\text{-}C_6H_4O_2{}^{\bullet -})$
Bond distances		
C1–O1	1.236 (1.222)*	1.304
C4–O2	1.236 (1.222)	1.255
C1–C2	1.479 (1.470)	1.443
C2–C3	1.338 (1.334)	1.373
C3–C4	1.479 (1.477)	1.449
C4–C5	1.479 (1.477)	1.458
C5–C6	1.338 (1.334)	1.362
C1–C6	1.479 (1.477)	1.444
Li–O1		2.141
Charge distribution		
O1	−0.251	−0.457
O2	−0.251	−0.315
C1	+0.260	+0.149
C2	−0.165	−0.136
C3	−0.164	−0.187
C4	+0.260	+0.210
C5	−0.164	−0.181
C6	−0.165	−0.247
Li	—	+0.641
H1	+0.16	+0.099
H2	+0.16	+0.134
H3	+0.16	+0.143
H4	+0.16	+0.144
Enthalpy of formation		
	−105.4	−99.1

* Results from van Bolhuis and Kiers:[8] errors ±0.003 Å.

Model structures

Table 3 presents the calculated bond distances, charge distributions and enthalpies of formation of $p\text{-}C_6H_4O_2$ and the monomeric lithium derivatives. The related bond angles are given in Scheme 1, which shows the numbering used. Both monomeric species are planar according to these models.

Table 3 shows that the calculated bond distances for $p\text{-}C_6H_4O_2$ are in good agreement with the experimental results. The results of the early X-ray studies of Trotter,[6] and the electron diffraction work of Swingle,[7] have been confirmed by low-temperature (−160 °C) crystallography by van Bolhuis and Kiers;[8] the values quoted in Table 3 are from this last investigation. The experimental bond angles [O–C–C 120.9, C–C(O)–C 118.2, C–C–C 120.9°; all ±0.1°] are also in reasonable agreement with those in Scheme 1. One small difference is that the slight deviation from planarity (0.3°) detected in the low-temperature X-ray crystallography is not predicted by the calculations. These points of agreement lend credibility to the calculated values for the other molecules involved, insofar as the structural parameters are concerned. We should note that, in contrast, the calculated enthalpy of formation of $p\text{-}C_6H_4O_2$ is −105.4 kJ mol^{-1}, which is significantly lower than the experimental value of −123 kJ mol^{-1}, suggesting that the thermodynamic parameters should be treated with caution.

The calculated values in Table 3 show that the formation of $Li^+(p\text{-}C_6H_4O_2{}^{\bullet -})$ results in the lengthening of C1–O1 to a value close to that found in other semiquininone complexes (average 1.29 Å). The Li–O bond distance is in the upper range of experimental values for a number of oligomeric Li–OR compounds,[1] and the bond is strongly polar, in keeping with the ESR results (see above). The C–O bond *para* to the lithium

Table 4 Calculated bond distances (Å) and charge distribution for $[Li^+(p\text{-}C_6H_4O_2{}^{\bullet -})]_2$

Bond distances

C1–O1	1.284	C4–C5	1.456
C4–O2	1.253	C5–C6	1.399
C1–C2	1.460	C1–C6	1.434
C2–C3	1.350	Li–O1	2.196
C3–C4	1.468		

Charge distribution		Change from monomer
O1	−0.431	+0.026
O2	−0.311	+0.004
C1	+0.227	+0.078
C2	−0.311	−0.175
C3	−0.257	−0.070
C4	+0.225	+0.015
C5	−0.159	+0.022
C6	−0.150	+0.097
Li	+0.564	−0.077
H1	+0.144	+0.045
H2	+0.156	+0.022
H3	+0.151	+0.008
H4	+0.152	+0.008

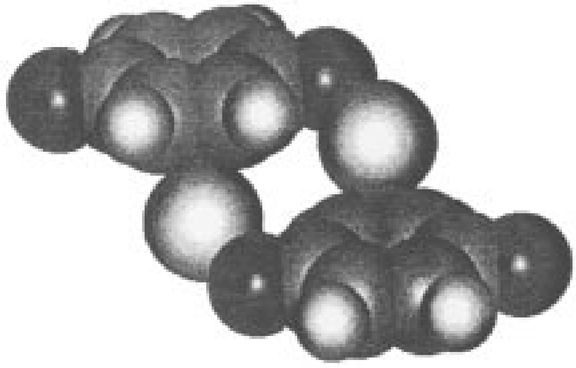

Fig. 3 The model structure of $[Li^+(p\text{-}C_6H_4O_2{}^{\bullet -})]_2$

loses some of the double-bond character seen in the parent quinone, lengthening by *ca.* 0.02 Å. The dimensions of the C_6 ring change slightly as the result of lithiation, the most important feature being some extension of the nominal C=C bonds. The small C–O–Li angle (93.5°) may indicate some interaction with the hydrogen H1 which shows the largest change in charge density on lithiation. Formation of the Li–O bond apparently removes the C_2 axis of $p\text{-}C_6H_4O_2$, with a consequent asymmetric charge distribution in the radical anion, both in the C_6 ring and at the hydrogen atoms. There is little evidence for any localisation of electron density within the ring itself.

These calculations refer to monomeric unsolvated molecules, and we have extended the calculations to the dimeric lithium compound $[Li^+(p\text{-}C_6H_4O_2{}^{\bullet -})]_2$. Fig. 3 shows the stereochemistry of the lowest-energy form of this molecule, and the relevant bond distances and atomic charges are in Table 4. The bond angles are only changed slightly on dimerisation (<1°), save for the Li–O–C bonds; the average value is 113° in plane, and 23° out of the ring plane, an increase of *ca.* 20°. Fig. 3 implies that the dimerisation of $Li^+(p\text{-}C_6H_4O_2{}^{\bullet -})$ does not involve the intuitive O1–Li···O2′ bonding, but rather an interaction between Li and the formally double bond at C2′–C3′. In fact the Li–O2′ distance is 4.215 Å, only slightly lower than Li–O1′ (4.296 Å), so that there are essentially no such interactions. In keeping with this the negative charge at O2 only changes by a negligible amount on dimerisation. Presumably the repulsive interaction between the π systems of the two rings prevents the close approach which would be required in the O1–Li···O2′ mode of bonding.

As noted above, the dimerisation of $Li^+(p\text{-}C_6H_4O_2{}^{\bullet -})$ involves the close approach of Li^+ to the C2′–C3′ bond, and the closest contact, Li–C3′, is only 2.40 Å. In keeping with this, the largest calculated changes in charge distribution (>±0.05) on dimerisation are (i) increases in the positive charge at C1 and C6, (ii) increases in the negative charge at C2 and C3, (iii) a decrease in the positive charge on Li, and (iv) a decrease in the negative charge at C6. The only significant difference in the hydrogen atoms is at H1, presumably a consequence of the elimination of the Li^+···H1 interaction identified for the monomer. In sum, the effects of the Li–C2′, C3′ interaction are reflected in charge reorganisation in the C_6 ring, and at the O–Li bond.

An interesting feature of these calculations is the estimation of ΔH_r for the process (5). The value found is −156.1 kJ, and it

$$2\,Li(sq) \longrightarrow [Li(sq)]_2 \qquad (5)$$

was also possible to calculate ΔH_f for the trimeric species $[Li^+(p\text{-}C_6H_4O_2{}^{\bullet -})]_3$. The value of −485.0 kJ mol^{-1} leads to $-H_r$ for process (6) at −187.7 kJ, which implies considerable stability

$$3\,Li(sq) \longrightarrow [Li(sq)]_3 \qquad (6)$$

for this entity. On the other hand, reaction (7) has $\Delta H_r = +46.5$

$$1.5\,[Li(sq)]_2 \longrightarrow [Li(sq)]_3 \qquad (7)$$

kJ, so that the formation of the trimer from the stable dimer is energetically unfavourable, which is in keeping with the absence of any ESR signal corresponding to triradical species in solution (see above). It should be emphasised that these calculations do not take account of any solvation forces, and in any case a value of ≈50 kJ derived from the difference of two larger numbers may be approaching the limits of the reliability of this feature of the calculations.

It is also possible to compare the results with one further aspect of the ESR spectroscopy. The *D* values reported in Table 2 result from a magnetic dipolar interaction between the spins in the two semiquinones in the dimer, and can be used to confirm the plausibility of the proposed structures. If we had a good idea of the spin distribution in the π-HOMO of the semiquinone the equations discussed earlier,[1] involving a summation of the dipolar terms over the dimer, could be used. Unfortunately, this information is lacking, and we have therefore resorted to a cruder model in which the spin is assumed to be centered in each ring, and the interaction between two point spins at distance *R* is then calculated. In this case the equation for *D* is (8). Since we can only measure the absolute magnitude

$$D = -3g^2\beta^2/2R^3 \qquad (8)$$

of *D* the negative sign in the equation is ignored. This procedure gives $R = 6.4$ Å for the $[Li^+(p\text{-}C_4H_4O_2{}^{\bullet -})]_2$ and $[Li^+(p\text{-}dtbsq^{\bullet -})]_2$ dimers and $R = 6.8$–7.5 Å for $[K^+(p\text{-}C_4H_4O_2{}^{\bullet -})]_2$ dimers. It is satisfying that our calculated structure for $[Li^+(p\text{-}C_4H_4O_2{}^{\bullet -})]_2$ gives a distance of 6.3 Å between similar carbon atoms on the two semiquinone rings.

Infrared spectroscopy

The infrared spectrum of $p\text{-}C_6H_4O_2$ in the carbonyl region has been the subject of some discussion, centered on the presence of two absorption bands at 1668 and 1655 cm^{-1}, by Brown[9] who attributes this effect to Fermi resonance (see also ref. 10). The infrared spectrum of $Li^+(p\text{-}C_6H_4O_2{}^{\bullet -})$ in either KBr or Nujol shows a single band at 1659 cm^{-1}. The interpretation of this is made uncertain by the fact that we do not know if the solid form of this compound is the monomer or the dimer, but the model structure for the dimer points to the presence of a

C=O, presumably giving rise to this absorption. We also find a new absorption at 1492 cm^{-1}, not seen in the parent *p*-quinone, and this is assigned to ν(C–O) of the Li–O–C group.

For *p*-dtbq, ν(C–O) is at 1655 cm^{-1} in KBr (*cf.* 1652 cm^{-1} reported for solution in CS_2[11]), but the lithium derivative shows no absorption in this region. There is a series of bands between 1480 and 1440 cm^{-1}, for both *p*-dtbq and Li$^+$(*p*-dtbsq$^{\cdot -}$); an absorption at 1448 cm^{-1} is only seen for the latter, and this may be ν(C–O) of the dimer (*cf.* ESR results discussed above). Carbonyl vibrations are also absent in the spectrum of Li$^+$-(*p*-nsq$^{\cdot -}$). In general, the infrared spectra in this region are compatible with the model structures, but cannot serve in themselves as a reliable guide.

Acknowledgements

The award of Research Grants (to B. R. M. and D. G. T.) from the Natural Sciences and Engineering Research Council of Canada is gratefully acknowledged.

References

1 M. A. Brown, B. R. McGarvey, A. Ozarowski and D. G. Tuck, *J. Am. Chem. Soc.*, 1996, **118**, 9691.
2 M. A. Brown, B. R. McGarvey, A. Ozarowski and D. G. Tuck, *J. Organomet. Chem.*, 1998, **550**, 165.
3 M. J. S. Dewar, E. G. Zoebisch, E. F. Healy and J. J. P. Stewart, *J. Am. Chem. Soc.*, 1985, **107**, 3902.
4 B. Venkataraman, B. G. Segal and G. K. Fraenkel, *J. Chem. Phys.*, 1959, **30**, 1006.
5 T. E. Gough, *Trans. Faraday Soc.*, 1966, **62**, 2321; I. C. P. Smith and A. Carrington, *Mol. Phys.*, 1967, **12**, 439.
6 J. Trotter, *Acta Crystallogr.*, 1960, **13**, 86.
7 S. M. Swingle, *J. Am. Chem. Soc.*, 1954, **76**, 1409.
8 F. van Bolhuis and C. Th. Kiers, *Acta Crystallogr., Sect. B*, 1978, **34**, 1015.
9 T. L. Brown, *Spectrochim. Acta*, 1963, **19**, 1065.
10 T. Anno and A. Sado, *Bull. Chem. Soc. Jpn.*, 1958, **31**, 734.
11 P. Yates, M. I. Ardao and L. F. Fieser, *J. Am. Chem. Soc.*, 1951, **73**, 650.

Received 2nd *January* 1998; *Paper* 8/00033F